Postprint of: J. Agric. Food Chem., Just Accepted Manuscript
DOI: 10.1021/acs.jafc.8b00880

Structural Characterization of Lignin from Maize (*Zea mays* L.) Fibers: Evidences for Diferuloylputrescine Incorporated into the Lignin Polymer in Maize Kernels

José C. del Río,[*†] Jorge Rencoret,[†] Ana Gutiérrez,[†] Hoon Kim,[‡§] and John Ralph[‡§]

[†]Instituto de Recursos Naturales y Agrobiología de Sevilla (IRNAS), CSIC, Avda. Reina Mercedes, 10, 41012-Seville, Spain

[‡]Department of Energy Great Lakes Bioenergy Research Center, the Wisconsin Energy Institute, University of Wisconsin-Madison, Madison, WI 53726, USA

[§]Department of Biochemistry, University of Wisconsin-Madison, Madison, WI 53706, USA

[*]Corresponding author: (Tel: +34 954624711; E-mail: delrio@irnase.csic.es)

ABSTRACT

The structure of the phenolic polymer in maize grain fibers, with 5.5% Klason lignin content, has been studied. For this, the milled wood lignin (MWL) and dioxane lignin (DL) preparations were isolated and analyzed. The data indicated that the lignin in maize fibers was syringyl-rich, mostly involved in β-aryl ether, resinol and phenylcoumaran substructures. 2D-NMR and derivatization followed by reductive cleavage (DFRC) also revealed the occurrence of associated ferulates together with trace amounts of *p*-coumarates acylating the γ-OH of lignin side-chains, predominantly on S-lignin units. More interesting was the occurrence of diferuloylputrescine, a ferulic acid amide, which was identified by 2D-NMR and comparison with a synthesized standard, that was apparently incorporated into this lignin. A phenylcoumaran structure involving a diferuloylputrescine coupled through 8−5′ linkages to another diferuloylputrescine (or to a ferulate or a guaiacyl lignin unit) was found, providing compelling evidence for its participation in radical coupling reactions. The occurrence of diferuloylputrescine in cell walls of maize kernels and other cereal grains appears to have been missed in previous works, perhaps due to the alkaline hydrolysis commonly used for compositional studies.

Keywords: Maize kernels, 2D-NMR, lignin monomers, hydroxycinnamoyl amides, ferulates

INTRODUCTION

Maize (*Zea mays* L.) fiber is the residue of the grain wet-milling process and comprises mostly the kernel outer seed coat (pericarp), together with some residual endosperm, and also contains testa and aleurone layers; it is similar to the maize bran, which arises from grain dry-milling.[1,2] Maize fiber is mostly composed of carbohydrate polymers, predominantly arabinoxylans and cellulose.[2] In addition, there are significant levels of ferulate esters linked to the cell-walls, together with lower amounts of *p*-coumarates.[3] Minor amounts of lignin have also been reported to occur in maize bran.[4−6]

In the cell walls of grasses, ferulate is mostly acylating the arabinosyl residues of (glucurono)arabinoxylans whereas *p*-coumarates are found similarly attached but also generally esterified by the γ-OH of the lignin side-chain.[7] Ferulate esters can participate in oxidative coupling reactions mediated by peroxidases, that may occur at the 4−*O*-, 5- or 8-positions forming ferulate dehydrodimers and higher dehydro-oligomers through different linkages (such as 8−*O*−4-, 4−*O*−5-, 8−8-, 5−5- and 8−5- linkages) thus creating cross-links between the arabinoxylan chains and providing recalcitrance to the cell wall. [8−16] In addition, ferulates and dehydrodiferulates can also cross-couple with monolignols helping to anchor and cross-link the lignin to the polysaccharide matrix and resulting in a highly recalcitrant lignin-hydroxycinnamate-carbohydrate complex.[8,9,11,12,14,17] Ferulates have therefore been proposed as initiation sites for lignification in grasses.[9,10]

Although most studies regarding the compositional and structural features of lignin in grasses have been devoted to the lignified stem tissues, several others have been aimed to investigate the lignin domain in cereal grains, including maize kernels.[5,14] Lapierre et al.[5] found

typical lignin structures in maize bran by using thioacidolysis, mainly comprising syringyl (**S**) units involved in β−*O*−4, β−1 and β−β linkages, and suggested that these lignin structures are tightly associated with heteroxylans by covalent linkages. Bunzel et al.[14] also detected the presence of 'authentic' lignin in maize bran by derivatization followed by reductive cleavage (DFRC), a degradative method that selectively cleaves β−*O*−4 linkages in lignin, as does thioacidolysis, also releasing predominantly syringyl lignin units. These authors also found 4−*O*−β and 8−β dimeric cross-coupled products of ferulates and coniferyl alcohol indicating the coupling of the carbohydrates to the lignin polymer via ferulates.

In this context, the aim of this study was to obtain additional insights into the nature of the lignin polymer in maize kernels. For this, the 'milled wood' lignin (MWL) and dioxane lignin (DL) preparations were isolated from maize kernel fibers (hereinafter simply called maize fibers) and subsequently analyzed by an array of analytical techniques, including pyrolysis-GC/MS, DFRC, 2D-NMR, and gel-permeation chromatography (GPC).

EXPERIMENTAL

Samples. The maize (*Zea mays* L.) fibers used for this study were the byproduct of the wet-milling process for maize starch processing and was kindly provided by Cargill, Inc. (Brazil). The air-dried samples were ground to pass 1 mm sieve using a cutting mill and then sequentially Soxhlet extracted with acetone (12 h), methanol (24h) and water (6 h), prior to the isolation of MWL and DL preparations. The Klason lignin content of the pre-extracted material was determined according to TAPPI method T222 om-88,[18] corrected for ash and protein content, and accounted for 5.5% ± 0.4 of dry-weight maize fiber (three replicates were used).

Lignin isolation and purification. Two different lignin preparations (MWL and DL) were obtained from extractive-free maize fibers. For the isolation of the MWL preparation, around 80 g of extractive-free material were finely ball-milled, extracted with dioxane-water (96:4, v/v), and the isolated lignin was then purified as described elsewhere.[19] The MWL yield represented around 15% of the Klason lignin content. For the extraction of DL preparation, around 100 g of extractive-free maize fibers were refluxed with 0.1 M HCl in dioxane:water (82:18, v/v) under nitrogen for 2 h. After the extractions the maize fibers were filtered and washed with dioxane:water (82:18, v/v). The filtrate was concentrated in a rotary evaporator at 40 °C, and then the lignin was precipitated at 4 °C in 1.5 L of cold distilled water under stirring. The precipitated lignin was then centrifuged and subsequently freeze-dried. The lignins were then Soxhlet-extracted with *n*-pentane to remove additional lipid extractives. The DL yield represented around 60% of the Klason lignin content.

Analytical pyrolysis. The maize kernel lignin preparations (~0.1 mg) were pyrolyzed at 500 ºC in a 3030 micro-furnace pyrolyzer (Frontier Laboratories Ltd., Fukushima, Japan) connected to a GC 7820A and a 5975 mass-selective detector (Agilent Technologies, Inc., Santa Clara, CA) using the conditions described previously.[20] For the pyrolysis in the presence of tetramethylammonium hydroxide (Py/TMAH), ~0.1 mg of lignin preparation was mixed with 1.0 µL of TMAH (25%, w/w, in methanol) prior to the pyrolysis. The released compounds were identified by comparison of their mass spectra with those from our own collection of standards and with those reported in the literature.

Derivatization followed by reductive cleavage (DFRC). DFRC degradation was performed according to the original procedure,[21] and the detailed explanation has been described elsewhere.[19] Around 10 mg of lignin preparation were treated with acetyl bromide in acetic acid

(8:92, v/v) at 50 ºC for 2 h, and then with 50 mg of powdered zinc for 40 min at room temperature. The lignin degradation products were acetylated with an acetic anhydride/pyridine solution (1:1, v/v) and dissolved in dichloromethane for subsequent analysis that were carried out in a Saturn 4000 GC-MS system (Varian, Walnut Creek, CA) using the conditions described previously.[20] Characteristic ions for the *cis*- and *trans*-coniferyl (*m/z* 222) and sinapyl (*m/z* 252) alcohol monomers (as their acetate derivatives), as well as for the *cis*- and *trans*-sinapyl dihydro-*p*-coumarates (*m/z* 400) (as their acetate derivatives), were collected to produce the reconstructed ion chromatograms.

Nuclear magnetic resonance (NMR) spectroscopy. Multidimensional NMR experiments (2D HSQC, 2D HMBC, 2D HSQC-TOCSY) were performed on an AVANCE III 500 MHz instrument (Bruker, Karlsruhe, Germany) fitted with a cryogenically cooled 5 mm TCI gradient probe with inverse geometry. Around 40 mg of lignin sample were dissolved in 0.75 mL of DMSO-d_6 and the spectra were recorded using the experimental conditions previously described.[20]

Gel permeation chromatography (GPC). GPC analysis of previously acetylated MWL was performed on a Prominence-i LC-2030 3D GPC system (Shimadzu, Kyoto, Japan) equipped with a photodiode array (PDA) detector and a PLgel MIXED-D column (Agilent Technologies, Stockport, United Kingdom), using the experimental conditions previously described.[20]

RESULTS AND DISCUSSION

Identification, composition and structure of lignin in maize kernels. The MWL and DL preparations obtained from the maize fibers were first analyzed by Py-GC/MS (Figure 1) that gave information about the composition of lignin and associated *p*-hydroxycinnamates. The identities and relative molar abundances of the released phenolic compounds are listed in Table 1. Pyrolysis released phenolic compounds derived mostly from *p*-hydroxycinnamates, and to a lower extent, from lignin. High amounts of 4-vinylguaiacol, **7**, and 4-vinylphenol, **8**, were released from both lignins, but, as occurs in grasses, they mostly arise from ferulates and *p*-coumarates after decarboxylation upon pyrolysis,[19,22,23] thus revealing the occurrence of important amounts of these *p*-hydroxycinnamates in the lignins. The MWL also showed important amounts of 4-vinylsyringol, **14**, mostly arising from sinapates after decarboxylation. Besides these vinyl phenolic compounds, the pyrograms also showed diagnostic compounds derived from the *p*-hydroxyphenyl (**H**), guaiacyl (**G**) and syringyl (**S**) lignin units such as guaiacol, **2**, 4-methylphenol, **3**, 4-methylguaiacol, **4**, 4-ethylguaiacol, **6**, syringol, **10**, 4-methylsyringol, **12**, 4-allylsyringol, **15**, *cis*-4-propenylsyringol, **16**, and *trans*-4-propenylsyringol, **17**, among others, that demonstrated the occurrence of typical lignin moieties in maize fibers. An estimation of the lignin composition was calculated without taking into consideration 4-vinylphenol, **8**, 4-vinylguaiacol, **7**, and 4-vinylsyringol, **14**, as these compounds mostly arise from *p*-hydroxycinnamates, and revealed the predominance of **S**-units (**S**/**G** ratios of 1.4 and 1.2 for MWL and DL, respectively) in the lignin from maize fibers (Table 1).

The occurrence of *p*-hydroxycinnamates (*p*-coumarates, ferulates, and sinapates) in the MWL and DL preparations isolated from maize fibers was confirmed by pyrolysis in the presence of tetramethylammonium hydroxide (TMAH), a reagent that prevents decarboxylation during pyrolysis and releases the respective methyl esters.[22,23] Py/TMAH released significant

amounts of the methylated derivatives of *p*-coumarate ***p*CA** (methyl *trans*-4-*O*-methyl-*p*-coumarate) and ferulate **FA** (methyl *trans*-4-*O*-methyl-ferulate), confirming their occurrence in these lignin preparations. The methyl derivative of sinapate **SA** (methyl *trans*-4-*O*-methyl-sinapate) was released in significant amounts only from the MWL but was absent in the DL preparation, as already indicated by Py-GC/MS results. In grasses, ferulates primarily acylate polysaccharides, i.e., are mostly esterified by polysaccharide units, generally at the C-5 hydroxyl of arabinosyl residues in arabinoxylans, and form dehydrodiferulates and higher dehydro-oligomers, as well as forming cross-coupled products with monolignols, whereas *p*-coumarates are largely esterified by the lignin γ-OH, and to a lower extent by polysaccharide moieties.[7] As indicated above, sinapates were only present in the MWL but were absent in the DL preparation, and they appear not to be part of the lignin in maize kernels.

The presence of lignin in maize fibers was further confirmed by DFRC, a chemical degradative method that selectively cleaves the β−*O*−4 linkages in β-ether units, similarly to thioacidolysis, but by a distinctly different mechanism, releasing the corresponding lignin monomers involved in these non-condensed units. DFRC can thus be used as another diagnostic technique to unambiguously detect the presence of 'true' lignin or lignin-like polymers in maize kernels. Figure 2 shows the reconstructed ion chromatogram (RIC) of the lignin units released upon DFRC from the MWL preparation. The lignin released the *cis*- and *trans*-isomers of guaiacyl (*c***G** and *t***G**), and syringyl (*c***S** and *t***S**) lignin monomers (as their acetylated derivatives), with a predominance of the **S**-units (**S**/**G** ratios of 1.7 and 1.8 for MWL and DL, respectively). Minor amounts of the conjugate sinapyl dihydro-*p*-coumarate (*c*$\mathbf{S_{DH}}$*p*$\mathbf{CA}$ and *t*$\mathbf{S_{DH}}$*p*$\mathbf{CA}$) were also released upon DFRC, indicating that, at least a part of the *p*-coumarates acylate the γ-OH of S-lignin units, as usually occurs in the lignins from grasses.[7] The release of **G**- and **S**-lignin units

upon DFRC supports the occurrence of a typical lignin polymer in maize kernels. It also demonstrates that β−*O*−4 alkyl aryl ether linkages involving **G**- and **S**-lignin units are present in the lignin preparations, establishing the existence of polymeric lignin in maize kernels, in agreement with the contentions from other authors.[5,14] Lapierre et al.[5] found typical β−*O*−4, β−1 and β−β lignin structures with a predominance of **S**-lignin units in maize bran by using thioacidolysis. Bunzel et al.[14] also detected the presence of lignin in cereal grains by using DFRC, where they found a predominance of **S**- over **G**-lignin units (**S**/**G** of 1.6) in the lignin from the insoluble dietary fiber from maize bran.

Additional information and revealing new insights about the composition and structure of the MWL and DL preparations isolated from maize fibers was obtained from 2D-HSQC-NMR (Figures 3 and 4). The aromatic region of the spectra (Figures 3C and 4C) gave information regarding the different lignin and *p*-hydroxycinnamate units present in the lignin preparations. The signal for the $C_{2,6}/H_{2,6}$ correlations from **S**-lignin units was clearly observed in this region of the spectrum whereas correlation signals for **G**-lignin units were barely detected but can be seen at lower contour levels, clearly indicating the occurrence of an **S**-rich lignin in maize kernels. The relative abundance of the **G**- and **S**-lignin units (as well as the rest of aromatic units) were estimated from the volume integrals of the respective signals and indicated S/G ratios of 2.1 and 1.9 for the MWL and DL, respectively. Signals from *p*-hydroxycinnamates were also present, including signals for *p*-coumarates (***p*CA**) and ferulates (**FA**), whereas the signal for sinapates (**SA**) were only detected in the MWL, confirming the results observed by Py-GC/MS and Py-TMAH. It should be noted that, although the association of ***p*CA** and **FA** is well established, **SA** is generally not associated with lignins. The aliphatic-oxygenated region of the spectra (Figures 3B and 4B) gave information about the different substructures, characterized by their diagnostic

187 inter-unit linkages, present in the lignin. In this region, typical signals from lignin substructures,
188 including the correlation signals from β-aryl ethers **A** (β–*O*–4′) and resinols **C** (β–β′), together
189 with lower levels of signals from phenylcoumarans **B** (β–5′), were clearly observed. Most
190 importantly, signals from structures involving ferulate moieties were readily observed in the
191 HSQC spectra, including signals for a structure (**B_{dFP}**) that presented similar correlations to those
192 reported for phenylcoumaran structures involving ferulate moieties.[17]

193 All of the analyses shown above (Py-GC/MS, Py-TMAH, DFRC, and 2D-NMR)
194 confirmed the existence of a lignin-polyphenolic domain in maize kernels, that is enriched in **S**-
195 units, which are mostly involved in β-aryl ethers **A**, phenylcoumarans **B**, and resinol **C**
196 substructures, and that also includes *p*-hydroxycinnamates, predominantly ferulates, involved in
197 4−*O*- and 8-coupled structures, as well as minor amounts of *p*-coumarates partially acylating the
198 γ-OH of the lignin side-chain.

199 **Identification of diferuloylputrescine in the lignin from maize kernels.** The 2D-HSQC-
200 NMR of the MWL and DL preparations (Figures 3 and 4) also showed an unexpected series of
201 signals that were unambiguously assigned here to the ferulic acid amides from
202 diferuloylputrescine (**dFP**). The aromatic region of the HSQC (Figures 3C and 4C) presented
203 characteristic signals for the C_7/H_7 and C_8/H_8 correlations of the unsaturated bonds of feruloyl
204 amides at δ_C/δ_H 138.6/7.30 (**dFP_7**) and 118.9/6.41 (**dFP_8**). The signal for the C_2/H_2 correlations
205 of feruloyl amides was also clearly observed at δ_C/δ_H 110.6/7.08 (**dFP_2**), whereas the signals
206 characteristic of the C_5/H_5, and C_6/H_6 correlations were in cluttered regions of the spectra but
207 those regions were consistent with correlations at 115.5/6.77 (**dFP_5**), and 121.2/6.96 (**dFP_6**), all
208 matching those previously reported for feruloyl amides.[24] The correlation signals for the aliphatic
209 methylene groups were readily observed in the aliphatic region of the HSQC spectra (Figures 3A

and 4A) at δ_C/δ_H 38.3/3.15 (**dFP**$_{10}$) and 26.6/1.45 (**dFP**$_{11}$). The definitive assignments of these signals were achieved by HSQC-TOCSY and HMBC experiments. The HSQC-TOCSY spectrum (Figure 5A) correlates the C_{10} and C_{11} carbons (δ_C 38.3 and 26.6, respectively) with the side-chain protons in the same spin system, including the amide N–H (at δ_H 7.98), and indicates the occurrence of two differentiated methylene groups. The HMBC experiment (Figure 5B) provides additional information regarding the long-range correlations of the methylene groups between them and with the N–H. Importantly, the spectrum also shows a correlation of C_{11} with what appears to be its own H_{11}, suggesting the symmetrical structure that corresponds to a 1,4-butanediamine (putrescine). Finally, Figure 6 shows the region of the HMBC spectrum correlating the carbonyl carbon (C_9) of the feruloyl amide at δ_C 165.0 with all protons within three bonds, namely the N–H and the H_{10} of the putrescine moiety, and the unsaturated protons (H_8 and H_7) of the ferulate side-chain. All these correlations are diagnostic for diferuloylputrescine (**dFP**). The HMBC of Figure 7 provides the remainder of the correlation signals that unambiguously demonstrate the occurrence of diferuloylputrescine in the lignin preparations isolated from maize fibers. The NMR signals exactly match those previously published for diferuloylputrescine, and particularly with the *E,E*-isomer,[25,26] and confirm those here with signals from authentically synthesized (*E,E*)-diferuloylputrescine. It must also be noted here that the C_7/H_7 and C_8/H_8 correlation signals for diferuloylputrescine were unequivocally present in the HSQC spectrum of the distiller's grain residues from the corn ethanol process,[27] although the signals were not assigned in that paper, additionally supporting the occurrence of diferuloylputrescine in maize kernels. However, it is important to point out that, as all the protons from the ferulates, and particularly those from the unsaturated moieties, are readily observed in the spectra, it is clear that these signals only represent the feruloyl amides that are

present as end-groups and not those that are expected to be coupled at 4−*O*-, 5- or 8-positions. A rough estimation of the abundance of **dFP** was obtained from volume integrals of the signal **dFP**$_2$ and indicated a relative content of 48% (in MWL) and 35% (in DL), referred to the total lignin units (G+S=100%).

Diferuloylputrescine itself is known to occur in the lipid extracts of maize kernels.[28] However, as the maize fibers studied here were subjected to exhaustive extraction with different solvents (acetone, methanol and water) aimed at removing all of these free amides and other extractives prior to lignin isolation, and the MWL and the DL preparations were additionally exhaustively washed with different organic solvents, it is possible to assume that the diferuloylputrescine moieties observed in these lignin preparations are linked to the cell walls of maize kernels by covalent bonds and do not correspond to residual free diferuloylputrescine molecules strongly associated to the cell walls. This assumption is also supported by the GPC of the MWL preparation that is quite homogeneous (M_w of 4900 g/mol; M_n of 3200 g/mol; with a very low polydispersity, M_w/M_n of 1.53) and does not include free non-polymerized diferuloylputrescine that might have been co-precipitated or co-extracted with the lignin-like polymer fraction. On the other hand, no traces of diferuloylputrescine (as its acetate derivative) could be detected among the DFRC degradation products, which seems to indicate that it could be present in polymeric form predominantly forming linkages that are not amenable to DFRC.

As occurs with ferulates, diferuloylputrescine is also expected to form dehydrodimers and higher dehydro-oligomers or be linked to other ferulates or to the lignin moiety. The occurrence of strong correlation signals for C_7/H_7 (at δ_C/δ_H 87.5/5.88, **B$_{dFP7}$**) and C_8/H_8 (δ_C/δ_H 55.6/4.21, **B$_{dFP8}$**) of an 8−5′ phenylcoumaran structure involving diferuloylputrescine (**B$_{dFP}$**) in the HSQC spectra (Figures 3B and 4B) clearly support this contention. These correlation signals are similar

to those published for ferulates involved in phenylcoumaran structures,[8,17] thus indicating the participation of ferulate moieties in this structure. The definitive assignment of this structure (**B_{dFP}**) was accomplished by long-range correlation experiments in the HMBC spectrum (Figure 8) that convincingly demonstrated that it corresponds to a phenylcoumaran structure involving one of the ferulate moieties of the diferuloylputrescine. It is clear from the HMBC spectrum that the carbonyl carbon (C_9) of the feruloyl amide in this phenylcoumaran structure (at δ_C 169.5) correlates with the N–H (at δ_H 8.37) and with the H_{10} of the aliphatic putrescine moiety, as well as with the H_7 and H_8 of the phenylcoumaran, confirming the involvement of diferuloylputrescine in this coupled structure. The rest of the correlation signals demonstrating the occurrence of this dehydrodimeric coupled structure **B_{dFP}** are also shown in Figure 8. The correlation signal for C_2/H_2 (at δ_C/δ_H 110.1/7.27, **B_{dFP2}**) and, at lower levels, the signal for C_6/H_6 (at δ_C/δ_H 118.3/6.73, **B_{dFP6}**), could also be clearly observed in the HSQC spectra of both MWL and DL preparations. The presence of this coupled structure provides compelling evidence for the participation of diferuloylputrescine in radical coupling reactions with other diferuloylputrescine, or with ferulates or lignin **G**-units, to be integrally incorporated and covalently linked to the cell wall. The occurrence of other coupled structures involving diferuloylputrescine, probably forming 5−5′, 8−*O*−4′ and other linkages, is highly suspected by the existence of other signals for feruloyl amides in the HMBC spectrum (Figure 9). Signals colored red in the spectrum correspond to the N–H correlations of the amide bond and are diagnostic for diferuloylputrescine. Correlations for the carbonyl carbon (C_9) of the amide group were found that corresponded to different structural types involving diferuloylputrescine. Besides the 4–*O*-, end-groups, and 8–5′ phenylcoumaran **B_{dFP}** structures that have already been assigned, signals for other structures were apparent in the HMBC spectrum (Figure 9). Signals

for 8−*O*−4′-coupled structures involving diferuloylputrescine were tentatively assigned by comparison with the relative shifts of the carbonyl groups in the HMBC spectrum of coupled structures from ferulates;[9,29] the correlation signals for the carbonyl carbon in 8−*O*−4′-coupled structures appear upfield in the spectrum, and only show correlation with H_7. Another coupled structure involving the 8-position of diferuloylputrescine (denoted as 8−?) was also observed but could not be definitively assigned. The authenticated occurrence of these other coupled structures involving diferuloylputrescine, particularly the definitive assignment of the 8−*O*−4′ coupled structure, is the subject of continuing investigations.

Hydroxycinnamic acid amides are a group of secondary metabolites that contribute to many developmental processes as well as plant responses against biotic and abiotic stress.[30,31] The polymerization of hydroxycinnamic acid amides, and particularly ferulic acid amides, in plant cell walls is a generally accepted mechanism of plant response to pathogen attack.[30] Hence, feruloyltryramine and feruloyloctopamine have been shown to be covalently linked to the cell wall in both natural and wound periderms of potato (*Solanum tuberosum*) tubers.[32] Feruloyltyramine has also been found incorporated into the lignins of tobacco plants.[33−35] The occurrence of diferuloylputrescine incorporated into the cell walls in maize kernels, and probably in other cereal grains, may have been missed or underestimated in previous compositional studies due to the limitations of analytical methodologies used to release dehydrodiferulates and higher dehydro-oligomers, mostly involving alkaline hydrolysis.[7,10−16]

The biosynthesis of diferuloylputrescine involves two different metabolic routes leading to the formation of their parent compounds, ferulic acid and putrescine, thus being a link between carbon and nitrogen metabolism. Whereas ferulic acid arises from the shikimate-derived phenylpropanoid pathway, as do the monolignols, the pathway for putrescine biosynthesis

involves a multiplicity of enzymes, with arginine decarboxylase as the key enzyme.[31,36] The condensation of feruloyl-CoA thioesters with putrescine is then catalyzed by the corresponding putrescine: feruloyl-CoA transferase.

Radical coupling of diferuloylputrescine and cross-coupling with ferulates, monolignols and the growing lignin polymer. Feruloyl amides are good substrates of peroxidase in vitro,[32,33] so they likely participate in a peroxidase-mediated polymerization to produce dehydrodimers and higher dehydro-oligomers by radical coupling reactions at their 4−*O*-, 5- and 8-positions, similarly to ferulates. Diferuloylputrescine is expected to be compatible with the radical coupling reactions that typify lignification and it is expected to participate in coupling and cross-coupling reactions with another diferuloylputrescine as well as with ferulates and monolignols and become integrally incorporated into the hydroxycinnamate-lignin network in the cell wall, as it has been shown above with the identification of the phenylcoumaran structure $\mathbf{B_{dFP}}$, as well as the tentative 8−*O*−4′ coupled structure, and others, involving diferuloylputrescine, and previously with the related tyramine ferulate analog.[34] The particular structure of diferuloylputrescine, with compatible phenolic groups at both ends of the molecule, can allow lignification to proceed in both directions forming covalent linkages at both ends of the molecule; additionally, as coupling is also possible at the 8-positions of the ferulate moiety, this implies that diferuloylputrescine can form branching points in the lignin polymer thus producing a highly cross-linked polymeric network. As occurs with ferulates, both of diferuloylputrescine ferulate moieties can be oxidized by peroxidases and/or laccases to form radicals that are stabilized by resonance (Figure 10). These radicals can eventually couple and cross-couple with another diferuloylputrescine molecule, or with ferulates and monolignols, forming a variety of dehydrodimers and higher dehydro-oligomers. In addition and as also occurs with ferulates, it

can be speculated that diferuloylputrescine, and also its dimers and higher oligomers, can also cross-couple with monolignols and the growing lignin polymer via radical coupling reactions, being integrally incorporated into the lignin polymer.

If diferuloylputrescine can be fully integrated into the lignin polymer in maize kernels then it can also be considered to be a lignin monomer, participating in coupling and cross-coupling reactions during lignification. Thus, diferuloylputrescine can potentially be added to the list of non-conventional phenolic lignin monomers recently discovered in plants, including phenolics from different biosynthetic pathways such as the flavone tricin,[19,37,38] the hydroxystilbene piceatannol,[20,39] and the related tyramine ferulate (feruloyltyramine).[34] These discoveries provide further evidence of the plasticity of the combinatorial radical process of lignification and continue to provide evidence that, as has been noted early on, "any phenolic transported to the lignifying zone of the cell wall can, subject to simple chemical compatibility, be incorporated into the polymer".[40]

Role of diferuloylputrescine in maize kernels and prospects for metabolic engineering to produce lignin polymers with new and improved properties. The so-called maize fiber essentially consists of the coat (pericarp) that covers the seed. Therefore, lignification of maize kernels plays an important role in seed protection. The incorporation of diferuloylputrescine into the lignin polymer in maize kernel can contribute to strengthening the cell walls, making them resistant to mechanical, chemical, and enzymatic attack. The particular structure of the diferuloylputrescine molecule, with a butane bridge linking two feruloyl amide moieties may also confer additional mechanical properties, such as plasticity, elasticity, flexibility, as well as hydrophobicity, to the seed kernel. Diferuloylputrescine, and presumably any end-group units,

347 can also provide antifungal and antimicrobial properties contributing to resistance to disease or
348 to pathogenic attack, thus further contributing to seed protection.

349 The incorporation of non-conventional monomers, not usually present in plant lignins, as
350 is the case on the diferuloylputrescine described here, can open up new ways to design and
351 engineer the structure of the lignin to produce polymers with new or improved properties, as
352 already considered with other phenolic compounds.[41–44] Metabolic engineering to introduce
353 diferuloylputrescine into the lignin of plants could provide lignins with special properties, such
354 as a conferring a higher degree of plasticity and flexibility. It could also provide a means to
355 increase disease resistance in plants by adding antifungal and antimicrobial properties, and may
356 provide a way of adding a stabilized source of N to soils. On the other hand, the particular
357 structure of the diferuloylputrescine, with two ferulates linked by amide bonds makes this
358 molecule potentially interesting for producing 'zip-lignins'.[45] The amide bond is susceptible to
359 cleavage, although requires fairly harsh acidic or basic conditions. Plants genetically engineered
360 to include diferuloylputrescine into their lignin polymers, thus introducing amide bonds in the
361 polymeric backbone which may make lignins more amenable to chemical depolymerization,
362 would parallel the successful introduction of other 'zip-molecules', such as monolignol ferulates,
363 into plants.[45–47] The incorporation of diferuloylputrescine into the lignin structure can alter and
364 modify the structure of the lignin polymer and may confer special properties, such as facilitating
365 lignin removal, altering mechanical properties (flexibility, elasticity), increasing hydrophobicity,
366 strengthening the cell wall, or adding antifungal/antimicrobial properties, among others.

367 In conclusion, the present work has demonstrated the occurrence of diferuloylputrescine,
368 a ferulic acid amide that appears to be integrally incorporated into the lignin polymer in maize
369 seed coats. The occurrence of diferuloylputrescine in maize kernels may have been overlooked in

previous studies due to the limitations of the analytical methodologies used to release dehydrodiferulates (and higher oligomers) that mostly involve alkaline hydrolysis. Diferuloylputrescine can be considered as a 'non-conventional' lignin monomer participating in coupling and cross-coupling reactions during lignification. This discovery has profound implications as this is another type of phenolic compound that can be considered for lignin modification. We contend that the incorporation of diferuloylputrescine into the lignin polymer in plants that normally do not contain it can open up new ways to design and engineer the lignin structure to produce lignin polymers with new or improved properties.

ACKNOWLEDGMENTS

We thank Prof. Jorge L. Colodette (University of Viçosa, Brazil) for providing the maize fibers used in this study. We also thank Matt Regner (University of Wisconsin-Madison) for synthesizing authentic diferuloylputrescine that will be described in forthcoming work. We finally thank Dr. Manuel Angulo (General Research Services, University of Seville, SGI-CITIUS) for performing the NMR analyses.

FUNDING SOURCES

JCdR, JRe, and AG were funded by the Spanish projects CTQ2014-60764-JIN and AGL2017-83036-R (financed by Agencia Estatal de Investigación, AEI, and Fondo Europeo de Desarrollo Regional, FEDER), and the CSIC project 2014-40E-097; JRa, and HK were funded by the DOE Great Lakes Bioenergy Research Center (DOE BER Office of Science DE-FC02-07ER64494 and DE-SC0018409).

REFERENCES

(1) Rose, D. J.; Inglett, G. E.; Liu, S. X. Utilisation of corn (*Zea mays*) bran and corn fiber in the production of food components. *J. Sci. Food Agric.* **2010**, *90*, 915–924.

(2) Gáspar, M.; Kálmán, G.; Réczey, K. Corn fiber as a raw material for hemicelluloses and ethanol production. *Process Biochem.* **2007**, *42*, 1135–1139.

(3) Akin, D. E.; Rigsby, L. L. Corn fiber: structure, composition, and response to enzymes for fermentable sugars and coproducts. *Appl. Biochem. Biotechnol.* **2008**, *144*, 59–68.

(4) Chanliaud, E.; Saulnier, L.; Thibault, J. –F. Alkaline extraction and characterization of heteroxylans from maize bran. *J. Cereal Sci.* **1995**, *21*, 195–203.

(5) Lapierre, C.; Pollet, B.; Ralet, M. –C.; Saulnier, L. The phenolic fraction of maize bran: evidence for lignin-heteroxylan association. *Phytochemistry* **2001**, *57*, 765–772.

(6) Chateigner-Boutin, A. L.; Ordaz-Ortiz, J. J.; Alvarado, C.; Bouchet, B.; Durand, S.; Verhertbruggen, Y.; Barrière, Y.; Saulnier, L. Developing pericarp of maize: a model to study arabinoxylan synthesis and feruloylation. *Front. Plant Sci.* **2016**, *7*, 1476.

(7) Ralph, J. Hydroxycinnamates in lignification. *Phytochemistry Rev.* **2010**, *9*, 65–83.

(8) Ralph, J.; Quideau, S.; Grabber, J. H.; Hatfield, R. D. Identification and synthesis of new ferulic acid dehydrodimers present in the grass cell walls. *J. Chem. Soc. Perkin Trans.* **1994**, *1*, 3485–3498.

(9) Ralph, J.; Grabber, J. H.; Hatfield, R. D. Lignin-ferulate cross-links in grasses: active incorporation of ferulate polysaccharide esters in ryegrass lignins. *Carbohydr. Res.* **1995**, *275*, 167–178.

(10) Hatfield, R. D.; Ralph, J.; Grabber, J. H. Cell wall cross-linking by ferulates and diferulates in grasses. *J. Sci. Food Agric.* **1999**, *79*, 403–407.

(11) Grabber, J. H.; Ralph, J.; Hatfield, R. D. Cross-linking of maize walls by ferulate dimerization and incorporation into lignin. *J. Agric. Food Chem.* **2000**, *48*, 6106–6113.

(12) Grabber, J. H.; Ralph, J.; Hatfield, R. D. Model studies of ferulate-coniferyl alcohol cross-product formation in primary maize walls: implications for lignification in grasses. *J. Agric. Food Chem.* **2002**, *50*, 6008–6016.

(13) Bunzel, M.; Ralph, J.; Kim, H.; Lu, F.; Ralph, S. A.; Marita, J. M.; Hatfield, R. D.; Steinhart, H. Sinapate dehydrodimers and sinapate-ferulate heterodimers in cereal dietary fiber. *J. Agric. Food Chem.* **2003**, *51*, 1427–1434.

(14) Bunzel, M.; Ralph, J.; Lu, F.; Hatfield, R. D.; Steinhart, H. Lignins and ferulate-coniferyl alcohol cross-coupling products in cereal grains. *J. Agric. Food Chem.* **2004**, *52*, 6496–6502.

(15) Bunzel, M.; Ralph, J.; Funk, C.; Steinhart, H. Structural elucidation of new ferulic acid-containing phenolic dimers and trimers isolated from maize bran. *Tetrahedron Lett.* **2005**, *46*, 5845–5850.

(16) Bunzel, M.; Ralph, J.; Brüning, P.; Steinhart, H. Structural identification of dehydrotriferulic and dehydrotetraferulic acids isolated from insoluble maize bran fiber. *J. Agric. Food Chem.* **2006**, *54*, 6409–6418.

(17) Zhang, A.; Lu, F.; Sun, R.; Ralph, J. Ferulate-coniferyl alcohol cross-coupled products formed by radical coupling reactions. *Planta* **2009**, *229*, 1099–1108.

(18) Tappi, *Tappi Test Methods 2004-2005*; Tappi Press: Norcoss, GA, 2004.

(19) del Río, J. C.; Rencoret, J.; Prinsen, P.; Martínez, Á. T.; Ralph, J.; Gutiérrez, A. Structural characterization of wheat straw lignin as revealed by analytical pyrolysis, 2D-NMR, and reductive cleavage methods. *J. Agric. Food Chem.* **2012**, *60*, 5922–5935.

(20) Rencoret, J.; Kim, H.; Evaristo, A. B.; Gutiérrez, A.; Ralph, J.; del Río, J. C. Variability in lignin composition and structure in cell walls of different parts of macaúba (*Acrocomia aculeata*) palm fruit. *J. Agric. Food Chem.* **2018**, *66*, 138–153.

(21) Lu, F.; Ralph, J. Derivatization followed by reductive cleavage (DFRC method), a new method for lignin analysis: protocol for analysis of DFRC monomers. *J. Agric. Food Chem.* **1997**, *45*, 2590–2592.

(22) del Río, J. C.; Martín, F.; González-Vila, F. J. Thermally assisted hydrolysis and alkylation as a novel pyrolytic approach for the structural characterization of natural biopolymers and geomacromolecules. *Trends Anal. Chem.* **1996**, *15*, 70–79.

(23) del Río, J. C.; Gutiérrez, A.; Rodríguez, I. M.; Ibarra, D.; Martínez, A. T. Composition of non-woody plant lignins and cinnamic acids by Py-GC/MS, Py/TMAH and FT-IR. *J. Anal. Appl. Pyrol.* **2007**, *79*, 39–46.

(24) da Costa, L.; Foston, M.; Bokade, V.; Azarpira, A.; Lu, F.; Ragauskas, A. J.; Ralph, J.; Dale, B.; Balan, V. Isolation and characterization of new lignin streams derived from extractive-ammonia (EA) pretreatment. *Green Chem.* **2016**, *18*, 4205–4215.

(25) Iwasa, K.; Takahashi, T.; Nishiyama, Y.; Moriyasu, M.; Sugiura, M.; Takeuchi, A.; Tode, C.; Tokuda, H.; Takeda, K. Online structural elucidation of alkaloids and other constituents in crude extracts and cultured cells of *Nandina domestica* by combination of LC-MS/MS, LC-NMR, and LC-CD analyses. *J. Nat. Prod.* **2008**, *71*, 1376–1385.

(26) Raj, M. K.; Balachandran, C.; Duraipandiyan, V.; Agastian, P.; Ignacimuthu, S.; Vijayakumar, A. Isolation of terrestribisamide from *Peltophorum pterocarpum* (DC.) Baker ex. K. Heyne and its antimicrobial, antioxidant, and cytotoxic activities. *Med. Chem. Res.* **2013**, *22*, 3823–3830.

(27) Xiang, Z.; Watson, J.; Tobimatsu, Y.; Runge, T. Film-forming polymers from distiller´s grains: structural material properties. *Ind. Crops Prod.* **2014**, *59*, 282–289.

(28) Moreau, R. A.; Nuñez, A.; Singh, V. Diferuloylputrescine and *p*-coumaroyl-feruloylputrescine, abundant polyamine conjugates in lipid extracts of maize kernels. *Lipids* **2001**, *36*, 839–844.

(29) Quideau, S.; Ralph, J. Lignin-ferulate cross-links in grasses. Part 4. Incorporation of 5–5-coupled dehydrodiferulate into synthetic lignin. *J. Chem. Soc. Perkin Trans.* **1997**, *1*, 2351–2358.

(30) Facchini, P. J.; Hagel, J.; Zulak, K. Z. Hydroxycinnamic acid amide metabolism: physiology and biochemistry. *Can. J. Bot.* **2002**, *80*, 577–589.

(31) Edreva, A, M.; Velikova, V. B.; Tsonev, T. D. Phenylamides in plants. *Russ. J. Plant Physiol.* **2007**, *54*, 278–301.

(32) Negrel, J.; Pollet, B.; Lapierre, C. Ether-linked ferulic acid amides in natural and wound periderms of potato tuber. *Phytochemistry* **1996**, *43*, 1195–1199.

(33) Negrel, J.; Jeandet, P. Metabolism of tyramine and feruloyltyramine in TMV inoculated leaves of *Nicotiana tabacum*. *Phytochemistry* **1987**, *26*, 2185–2190.

(34) Ralph, J.; Hatfield, R. D.; Piquemal, J.; Yahiaoui, N.; Pean, M.; Lapierre, C.; Boudet, A. M. NMR characterization of altered lignins extracted from tobacco plants down-regulated for lignification enzymes cynnamyl-alcohol dehydrogenase and cynnamoyl-CoA reductase. *Proc. Natl. Acad. Sci. USA* **1998**, *95*, 12803–12808.

(35) Kaur, H.; Shaker, K.; Heinzel, N.; Ralph, J.; Gális, I.; Baldwin, I. T. Environmental stresses of field growth allow cinnamyl alcohol dehydrogenase-deficient *Nicotiana attenuata* plants to compensate for their structural deficiencies. *Plant Physiol.* **2012**, *159*, 1545–1570.

(36) Page, A. F.; Cseke, L. J.; Minocha, R.; Turlapati, S. A.; Podila, G. K.; Ulanov, A.; Li, Z.; Minocha, S. C. Genetic manipulation of putrescine biosynthesis reprograms the cellular transcriptome and the metabolome. *BMC Plant Biol.* **2016**, *16*, 113.

(37) Lan, W.; Lu, F.; Regner, M.; Zhu, Y.; Rencoret, J.; Ralph, S. A.; Zakai, U. I.; Morreel, K.; Boerjan, W.; Ralph, J. Tricin, a flavonoid monomer in monocot lignification. *Plant Physiol.* **2015**, *167*, 1284–1295.

(38) Lan, W.; Morreel, K.; Lu, F.; Rencoret, J.; del Río, J. C.; Vooren, W.; Vermerris, W.; Boerjan, W.; Ralph, J. Maize tricin-oligolignol metabolites and their implications for monocot lignification. *Plant Physiol.* **2016**, *171*, 810–820.

(39) del Río, J. C.; Rencoret, J.; Gutiérrez, A.; Kim, H.; Ralph, J. Hydroxystilbenes are monomers in palm fruit endocarp lignins. *Plant Physiol.* **2017**, *174*, 2072–2082.

(40) Ralph, J.; Brunow, G.; Harris, P. J.; Dixon, R. A.; Schatz, P. F.; Boerjan, W. Lignification: Are lignins biosynthesized via simple combinatorial chemistry or via proteinaceous control and template replication? In *Recent Advances in Polyphenol Research, Vol 1*; Daayf, F., El Hadrami, A., Adam, L., Ballance, G. M., Eds; Wiley-Blackwell Publishing: Oxford, 2008; p 36.

(41) Grabber, J. H.; Schatz, P. F.; Kim, H.; Lu, F.; Ralph, J. Identifying new lignin bioengineering targets: 1. Monolignol-substitute impacts on lignin formation and cell wall fermentability. *BMC Plant Biol.* **2010**, *10*, 114.

(42) Vanholme, R.; Morreel, K.; Ralph, J.; Boerjan, W. Lignin engineering. *Curr. Opin. Plant Biol.* **2008**, *11*, 278–285.

(43) Vanholme, R.; Morreel, K.; Darrah, C.; Oyarce, P.; Grabber, J. H.; Ralph, J.; Boerjan, W. Metabolic engineering of novel lignin in biomass crops. *New Phytol.* **2012**, *196*, 978–1000.

(44) Mottiar, Y.; Vanholme, R.; Boerjan, W.; Ralph, J.; Mansfield, S. D. Designer lignins: harnessing the plasticity of lignification. *Curr. Opin. Biotechnol.* **2016**, *37*, 190–200.

(45) Wilkerson, C. G.; Mansfield, S. D.; Lu, F.; Withers, S.; Park, J. -Y.; Karlen, S. D.; Gonzales-Vigil, E.; Padmakshan, D.; Unda, F.; Rencoret, J.; Ralph, J. Monolignol ferulate transferase introduces chemically labile linkages into the lignin backbone. *Science* **2014**, *9*, 2510–2516.

(46) Zhou, S.; Runge, T., Karlen, S. D.; Ralph, J.; Gonzales-Vigil, E.; Mansfield, S. D. Chemical pulping advantages of zip-lignin hybrid poplar. *ChemSusChem* **2017**, *10*, 3565–3573.

(47) Kim, K. H.; Dutta, T.; Ralph, J.; Mansfield, S. D.; Simmons, B. A.; Singh, S. Impact of lignin polymer backbone esters on ionic liquid pretreatment of poplar. *Biotechnol. Biofuels* **2017**, *10*, 101.

(48) Kim, H. K.; Padmakshan, D.; Li, Y.; Rencoret, J.; Hatfield, R. D.; Ralph, J. Characterization and elimination of undesirable protein residues in plant cell wall materials for enhancing lignin analysis by solution-state Nuclear Magnetic Resonance spectroscopy. *Biomacromolecules* **2017**, *18*, 4184–4195.

FIGURE LEGENDS

Figure 1. Py-GC/MS chromatograms of (A) MWL and (B) DL preparations isolated from maize fibers. The identities and relative abundances of the lignin-derived phenolic compounds released are listed in Table 1.

Figure 2. Reconstructed Ion Chromatogram (sum of the ions *m/z* 222+252+400) of the DFRC degradation products released from the MWL lignin preparation isolated from maize fibers. *c***G**, *t***G**, *c***S** and *t***S** are the *cis*- and *trans*-coniferyl (**G**) and sinapyl (**S**) alcohol monomers (as their acetate derivatives); $c\mathbf{S}_{\mathbf{DH}p\mathbf{CA}}$ and $t\mathbf{S}_{\mathbf{DH}p\mathbf{CA}}$ are the *cis*- and *trans*-sinapyl dihydro-*p*-coumarates (as their acetate derivatives).

Figure 3. 2D HSQC NMR spectrum (in DMSO-d_6) of the MWL preparation isolated from maize fibers. (A) Aliphatic (δ_C/δ_H 23−43/0.7−4.0); (B) aliphatic-oxygenated (δ_C/δ_H 50−90/2.8−6.0); and (C) aromatic (δ_C/δ_H 100−148/6.1−7.8) regions. Main structures found are **A**: β–*O*–4′ alkyl-aryl ethers; **B**: β–5′ phenylcoumarans; $\mathbf{B_{dFP}}$: 8–5′ phenylcoumarans involving diferuloylputrescine; **C**: resinols; ***p*CA**: *p*-coumarates; ***p*CA′**: *p*-coumaroyl amides; **FA**: ferulates; **SA**: sinapates; **S**: syringyl units; **dFP**: diferuloylputrescine. Protein residues were assigned according to the literature,[48] and are denoted as follows: phenylalanine (**Phe**); tyrosine (**Tyr**). The percentages for the various lignin inter-unit linkages (**A**, **B**, $\mathbf{B_{dFP}}$, **C**) were estimated from volume integration and total 100%. The percentages for the various lignin units (**S**, **G**) were estimated from volume integration; the relative abundances of ***p*CA**, **FA**, **SA** and **dFP** are referred as a percentage of the total lignin units (S + G = 100%).

Figure 4. 2D HSQC NMR spectrum (in DMSO-d_6) of the DL preparation isolated from maize fibers. (A) Aliphatic (δ_C/δ_H 23−43/0.7−4.0); (B) aliphatic-oxygenated (δ_C/δ_H 50−90/2.8−6.0);

and (C) aromatic (δ_C/δ_H 100−148/6.1−7.8) regions. Main structures found are depicted in Figure 3, and are: **A**: β–*O*–4′ alkyl-aryl ethers; **B**: β–5′ phenylcoumarans; $\mathbf{B_{dFP}}$: 8–5′ phenylcoumarans involving diferuloylputrescine; **C**: resinols; ***p*CA**: *p*-coumarates; ***p*CA′**: *p*-coumaroyl amides; **FA**: ferulates; **G**: guaiacyl units; **S**: syringyl units; **dFP**: diferuloylputrescine. Protein residues were assigned according to the literature,[48] and are denoted as follows: phenylalanine (**Phe**); tyrosine (**Tyr**). The percentages for the various lignin inter-unit linkages (**A**, **B**, $\mathbf{B_{dFP}}$, **C**) were estimated from volume integration and total 100%. The percentages for the various lignin units (**S**, **G**) were estimnated from volume integration; the relative abundances of ***p*CA**, **FA**, and **dFP** are referred as a percentage of the total lignin units (S + G = 100%).

Figure 5. (A) Partial $^{1}H–^{13}C$ total correlation (HSQC-TOCSY) spectrum (δ_C/δ_H 24−41/0.5−8.5) of the MWL preparation showing the main correlations for the aliphatic side-chains (C_{10} and C_{11}) and the N–H of diferuloylputrescine. (B) Section of the long-range $^{1}H–^{13}C$ correlation HMBC spectrum (δ_C/δ_H 24−41/0.5−8.5) of the MWL preparation showing the main correlations for the aliphatic side-chains and the N–H of the diferuloylputrescine. Signals colored red correspond to the N–H correlations of the amide bond.

Figure 6. (A) Section of the HMBC spectrum (δ_C/δ_H 163−168/2.0−8.5) of the MWL preparation isolated from maize fibers showing the main correlations for the carbonyl carbons of diferuloylputrescine at δ_C 165.0. (B) Appropriate sections of the HSQC spectrum showing the C_{10}/H_{10} correlations of the 1,4-butanediamine moiety (δ_C 36−40) and the C_7/H_7 and C_8/H_8 correlations of the feruloyl units (δ_C 137−140 and 117−120, respectively). Signals colored red correspond to the N–H correlations of the amide bond.

563 **Figure 7.** Partial $^{1}H–^{13}C$ long-range correlation (HMBC) spectrum (δ_C/δ_H 100−170/6.3−7.5) of
564 the MWL preparation from maize fibers showing the main correlations for the aromatic and
565 unsaturated carbons in diferuloylputrescine (**dFP**).

566 **Figure 8.** HMBC spectrum (δ_C/δ_H 20−175/1.0−8.7) of the MWL preparation from maize fibers
567 showing the main correlations for the 8–5′ phenylcoumaran structure $\mathbf{B_{dFP}}$ involving
568 diferuloylputrescine (**dFP**). Signals colored red correspond to the N–H correlations of the amide
569 bond.

570 **Figure 9.** Partial HMBC spectrum of the MWL preparation from maize fibers showing the
571 correlations of the carbonyl carbon (C_9) of the diferuloylputrescine-derived units with protons
572 that are within three-bonds. Signals colored red correspond to the N–H correlations of the amide
573 bond, diagnostic for diferuloylputrescine in different structures.

574 **Figure 10.** (A) Oxidative radicalization resulting from one-electron oxidation of
575 diferuloylputrescine stabilized by delocalization; resonance forms are displayed in which the
576 single-electron density is shown to localize at the 4–*O*-, 5- and 8-positions. The other ferulate
577 moiety can also be oxidized to a radical in the same manner, allowing it to also undergo
578 independent radical coupling. (B) Dehydrodimerization products arising from oxidative coupling
579 of diferuloylputrescine at 4–*O*-, 5- and 8-positions.

Table 1. Identities and Relative Molar Abundances of the Lignin- and Hydroxycinnamate-Derived Phenolic Monomeric Compounds Released after Py-GC/MS of the MWL and DL Preparations Isolated from Maize Fibers.

No.	Compound	MWL (%)	DL (%)	Origin
1	phenol	3.4	3.4	**H**
2	guaiacol	6.1	7.9	**G**
3	4-methylphenol	2.4	5.1	**H**
4	4-methylguaiacol	3.4	7.0	**G**
5	4-ethylphenol	0.9	2.2	**H**
6	4-ethylguaiacol	3.0	4.3	**G**
7	4-vinylguaiacol	34.3	32.3	**G/FA**
8	4-vinylphenol	8.2	11.5	**H/*p*CA**
9	eugenol	0.3	0.2	**G**
10	syringol	6.8	5.6	**S**
11	*trans*-isoeugenol	0.6	0.6	**G**
12	4-methylsyringol	2.8	4.5	**S**
13	4-ethylsyringol	1.4	1.8	**S**
14	4-vinylsyringol	19.0	2.4	**S/SA**
15	4-allyl-syringol	1.2	1.2	**S**
16	*cis*-4-propenylsyringol	0.7	1.0	**S**
17	*trans*-4-propenylsyringol	3.5	5.6	**S**
18	acetosyringone	0.4	1.0	**S**
19	syringylacetone	1.0	1.5	**S**
20	propiosyringone	0.5	0.8	**S**
%**H***=		17	20	
%**G***=		34	37	
%**S***=		49	43	
S/G*=		1.4	1.2	

*estimated without using 4-vinylphenol, **8**, 4-vinylguaiacol, **7**, and 4-vinylsyringol, **14**.

H: *p*-hydroxyphenyl units; **G**: guaiacyl units; **S**: syringyl units; ***p*CA**: *p*-coumarates; **FA**: ferulates; **SA**: sinapates

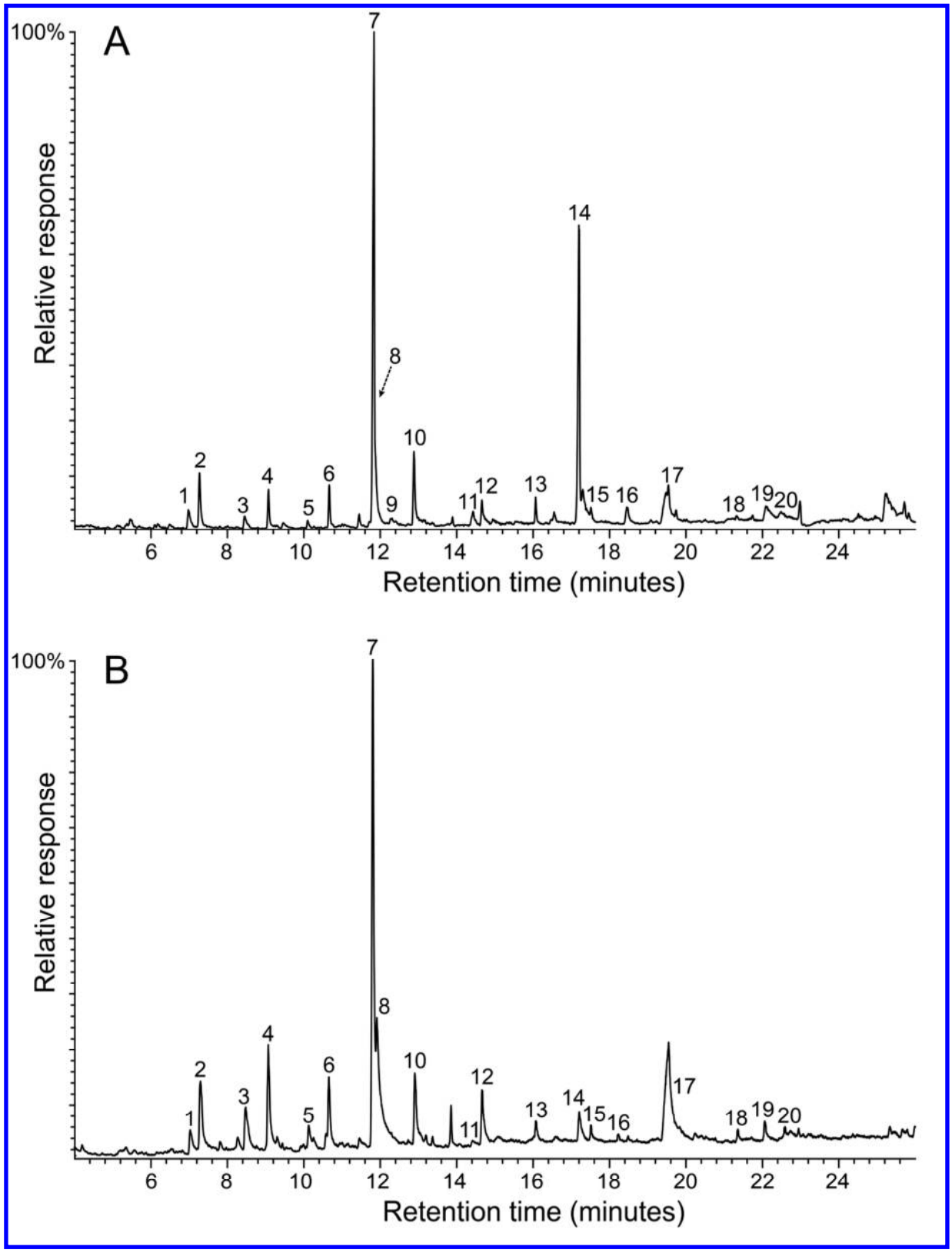
A
100%
Relative response
Retention time (minutes)
B
100%
Relative response
Retention time (minutes)

Figure 1

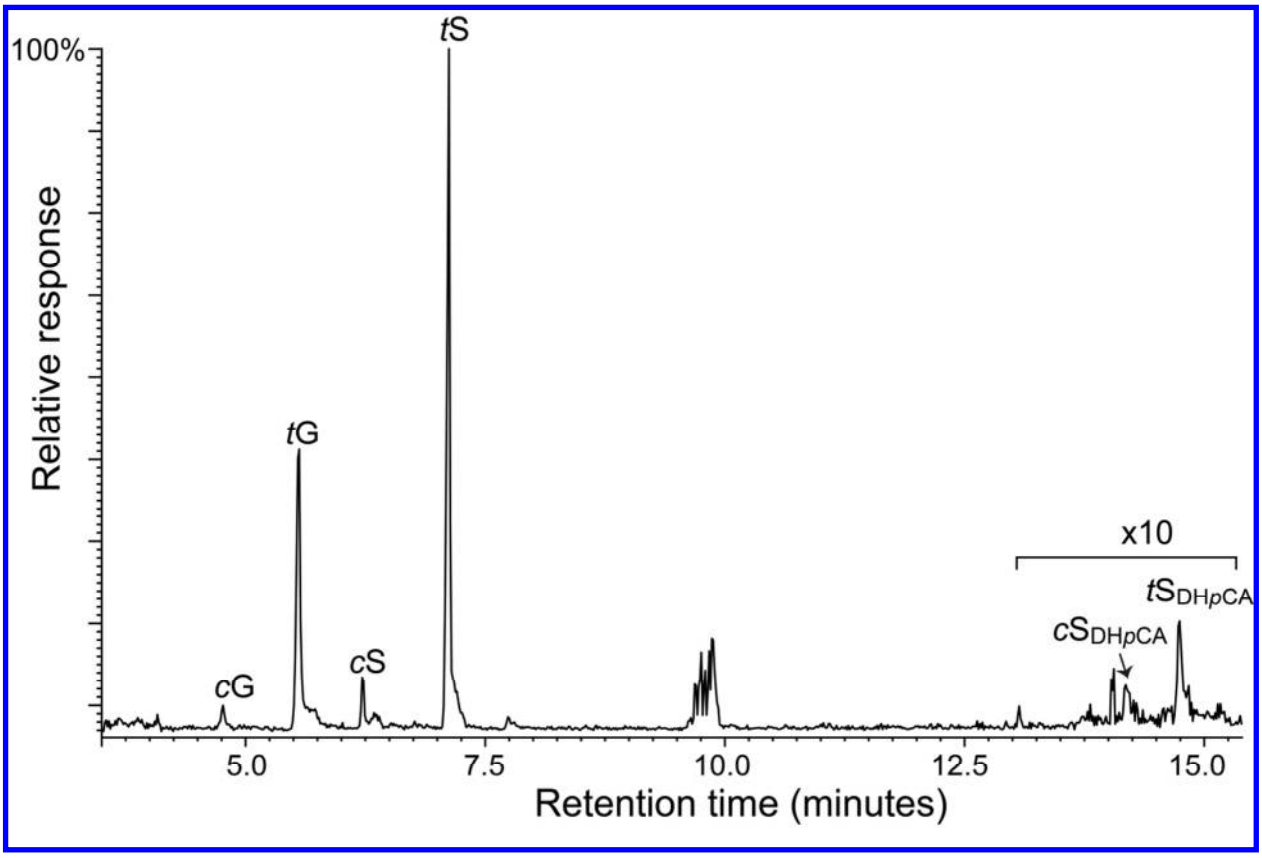
100%
Relative response
tS
tG
cS
cG
x10
tSDHpCA
cSDHpCA
5.0
7.5
10.0
12.5
15.0
Retention time (minutes)

Figure 2

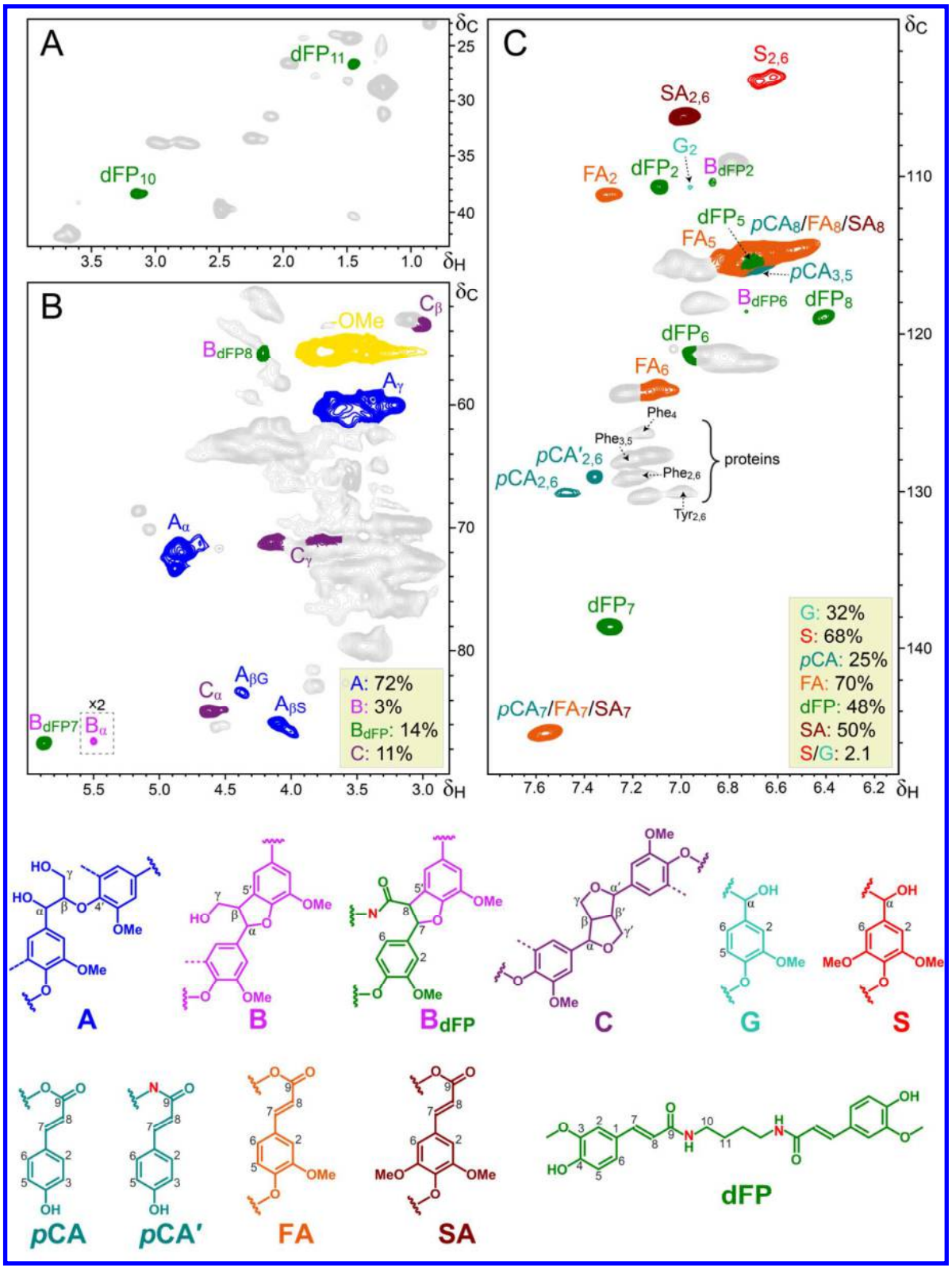
A
dFP11
dFP10
δC
δH
B
-OMe
Cβ
BdFP8
Aγ
Aα
Cγ
Cα
AβG
AβS
x2
BdFP7
Bα
A: 72%
B: 3%
BdFP: 14%
C: 11%
C
S2,6
SA2,6
G2
FA2
dFP2
BdFP2
dFP5
pCA8/FA8/SA8
FA5
pCA3,5
BdFP6
dFP8
dFP6
FA6
Phe4
Phe3,5
pCA'2,6
pCA2,6
Phe2,6
Tyr2,6
proteins
dFP7
pCA7/FA7/SA7
G: 32%
S: 68%
pCA: 25%
FA: 70%
dFP: 48%
SA: 50%
S/G: 2.1
A
B
BdFP
C
G
S
pCA
pCA'
FA
SA
dFP

Figure 3

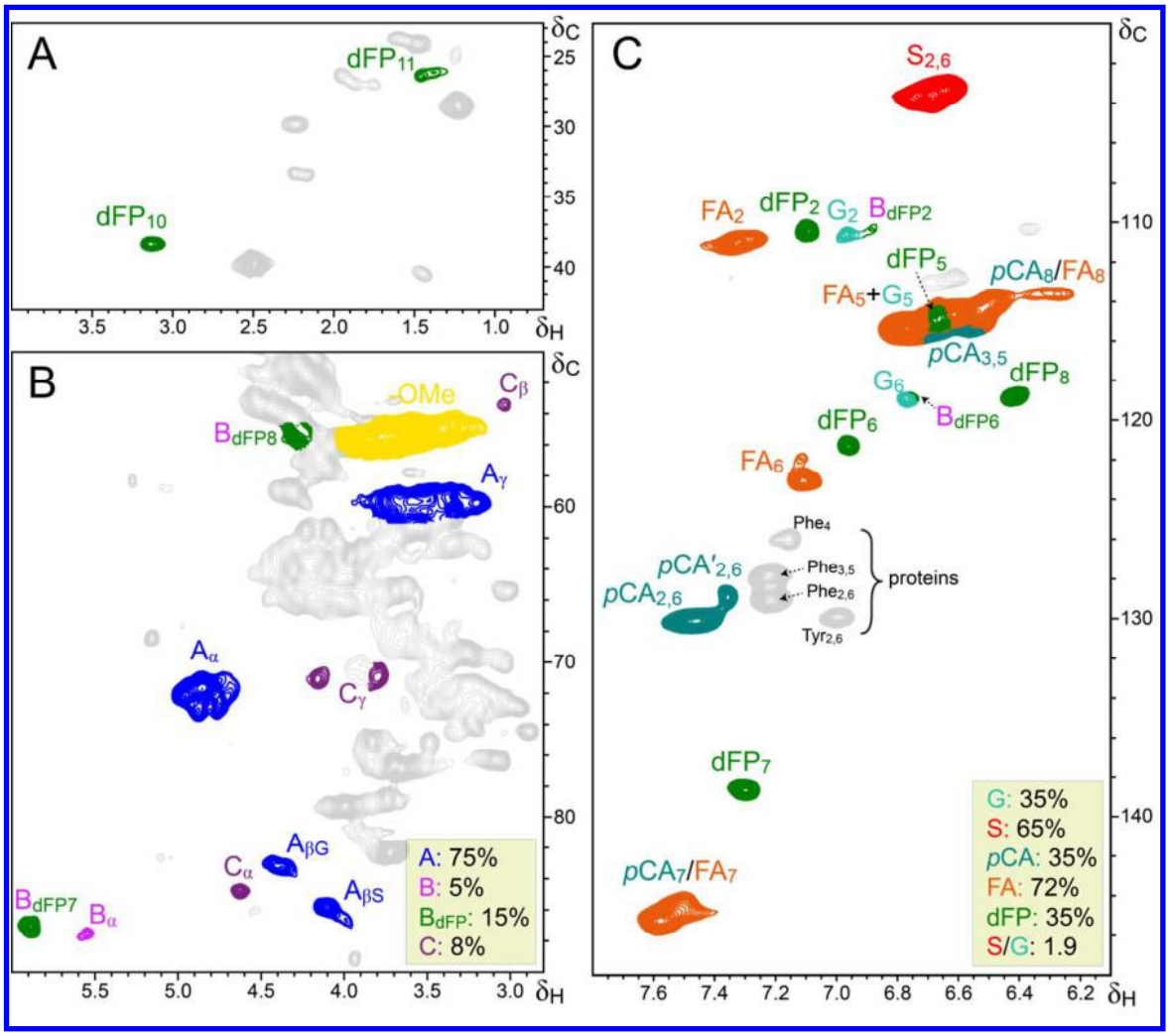
A
dFP11
dFP10
δC
δH
B
-OMe
Cβ
BdFP8
Aγ
Aα
Cγ
AβG
Cα
AβS
BdFP7
Bα
A: 75%
B: 5%
BdFP: 15%
C: 8%
C
S2,6
FA2
dFP2
G2
BdFP2
dFP5
pCA8/FA8
FA5+G5
pCA3,5
dFP8
G6
BdFP6
dFP6
FA6
Phe4
pCA'2,6
Phe3,5
pCA2,6
Phe2,6
proteins
Tyr2,6
dFP7
pCA7/FA7
G: 35%
S: 65%
pCA: 35%
FA: 72%
dFP: 35%
S/G: 1.9

Figure 4

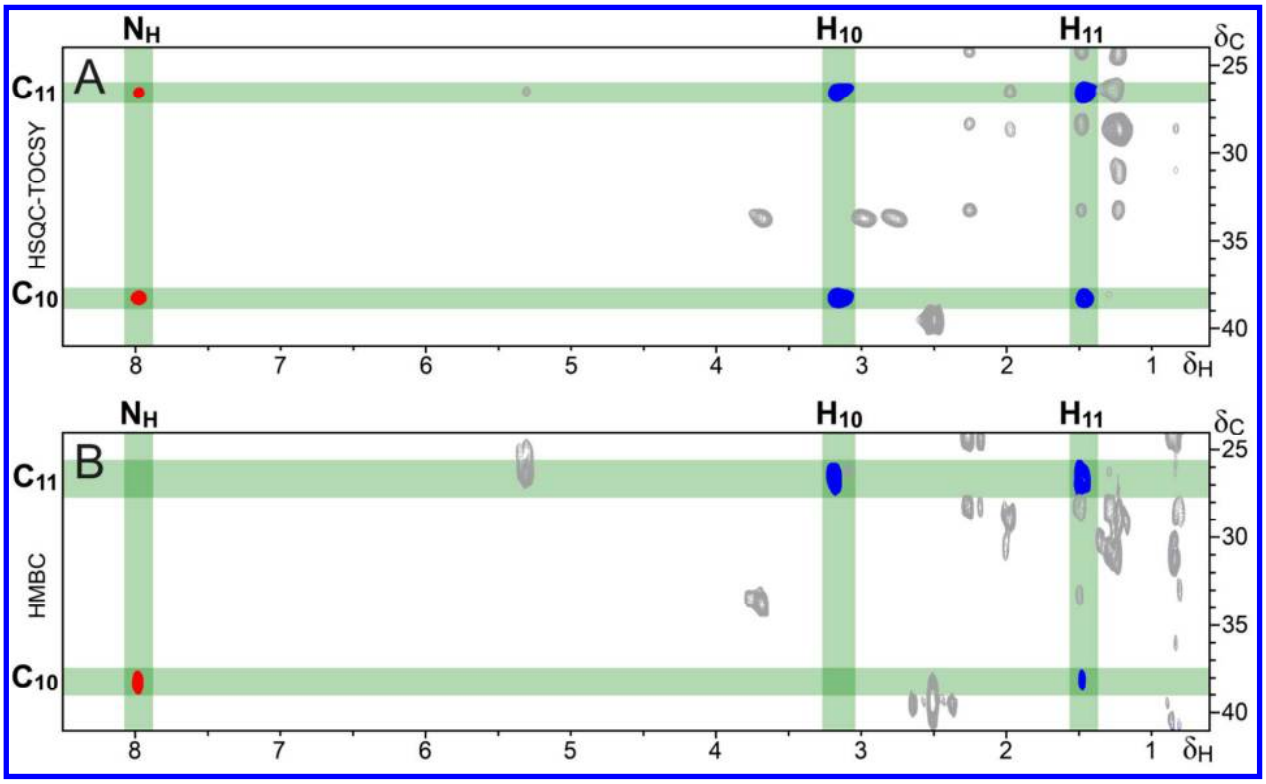
A
B
HSQC-TOCSY
HMBC
N_H
H_{10}
H_{11}
C_{11}
C_{10}
δ_C
δ_H
25
30
35
40
8
7
6
5
4
3
2
1

Figure 5

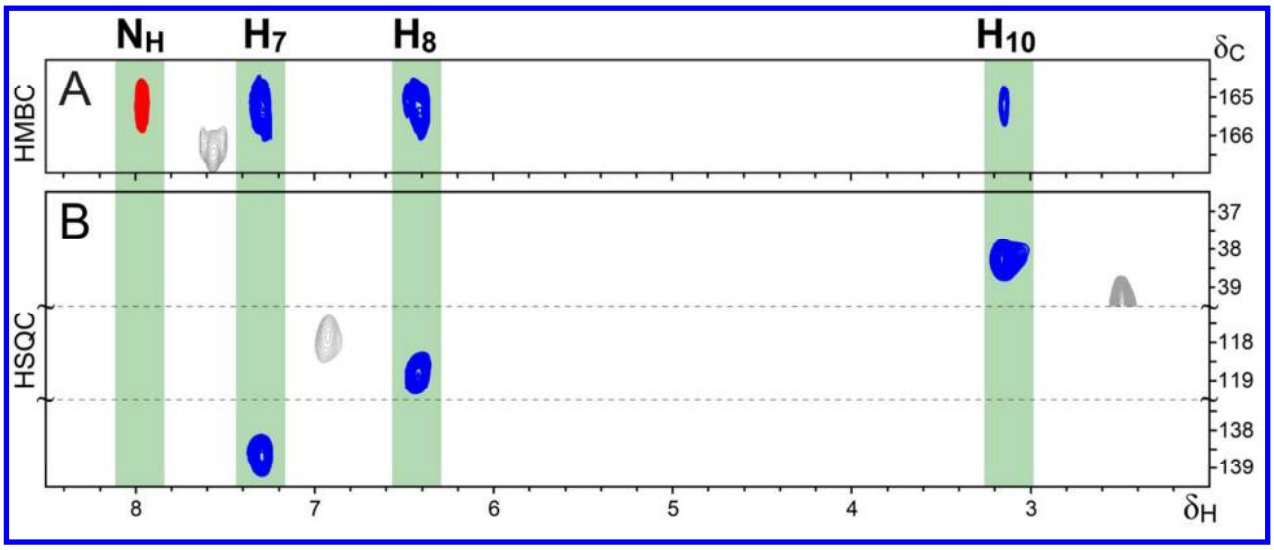
NH
H7
H8
H10
δC
A
HMBC
165
166
B
HSQC
37
38
39
118
119
138
139
8
7
6
5
4
3
δH

Figure 6

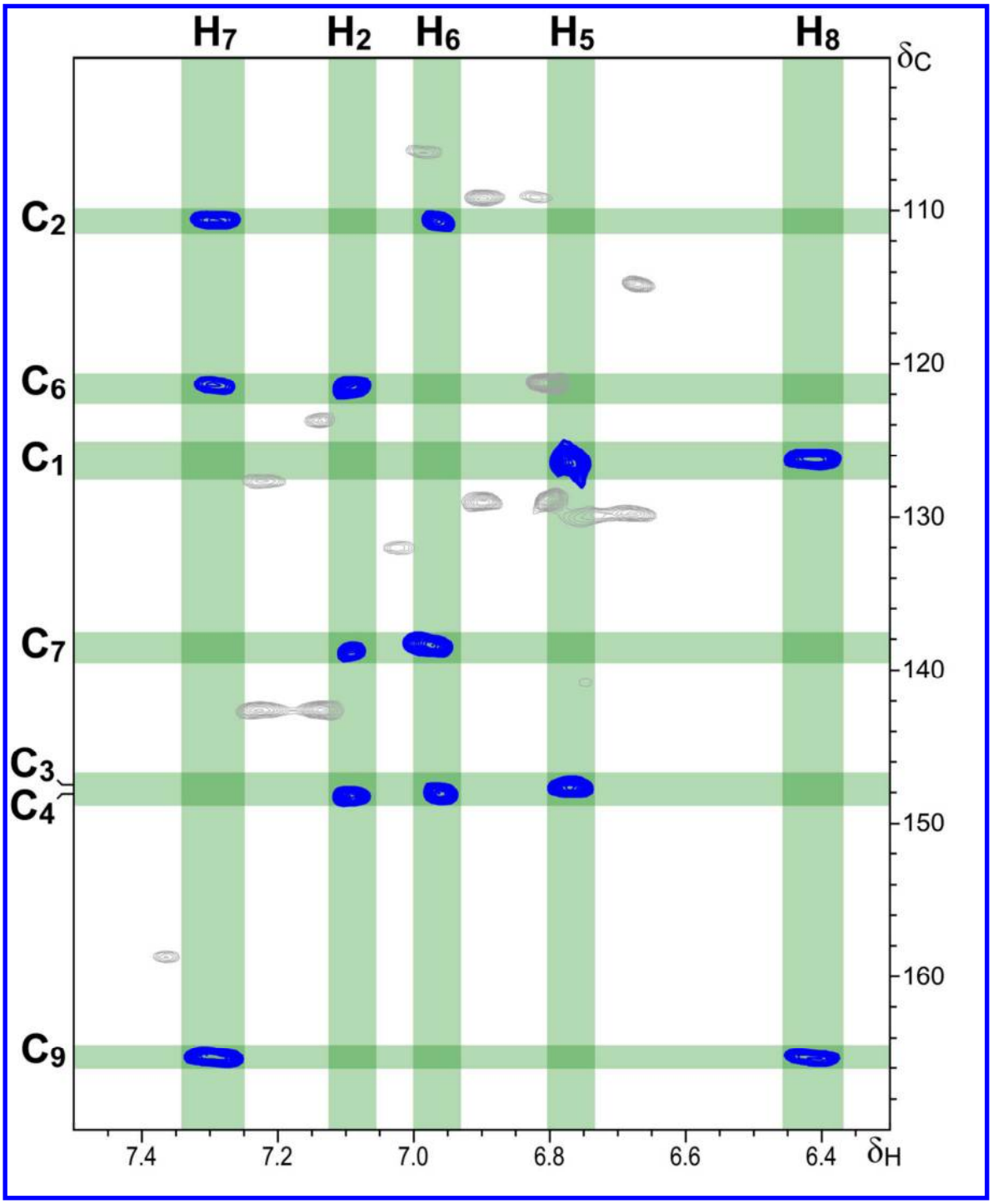
H7
H2
H6
H5
H8
δC
C2
C6
C1
C7
C3
C4
C9
110
120
130
140
150
160
7.4
7.2
7.0
6.8
6.6
6.4
δH

Figure 7

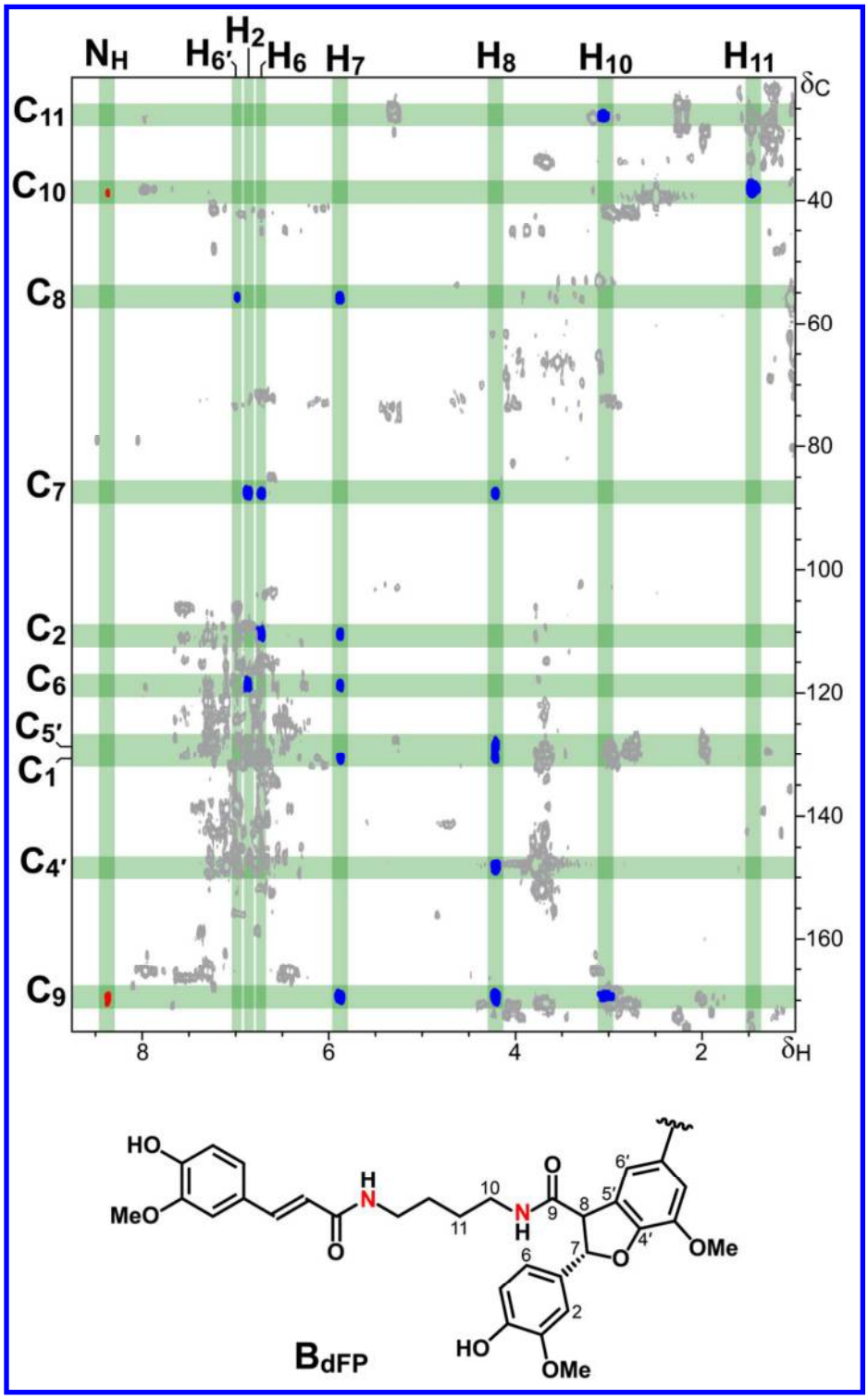
NH
H6′
H2
H6
H7
H8
H10
H11
δC
C11
C10
C8
C7
C2
C6
C5′
C1
C4′
C9
40
60
80
100
120
140
160
8
6
4
2
δH
HO
MeO
H
N
O
10
11
N
H
O
9
8
5′
6′
4′
OMe
O
7
6
2
HO
OMe
BdFP

Figure 8

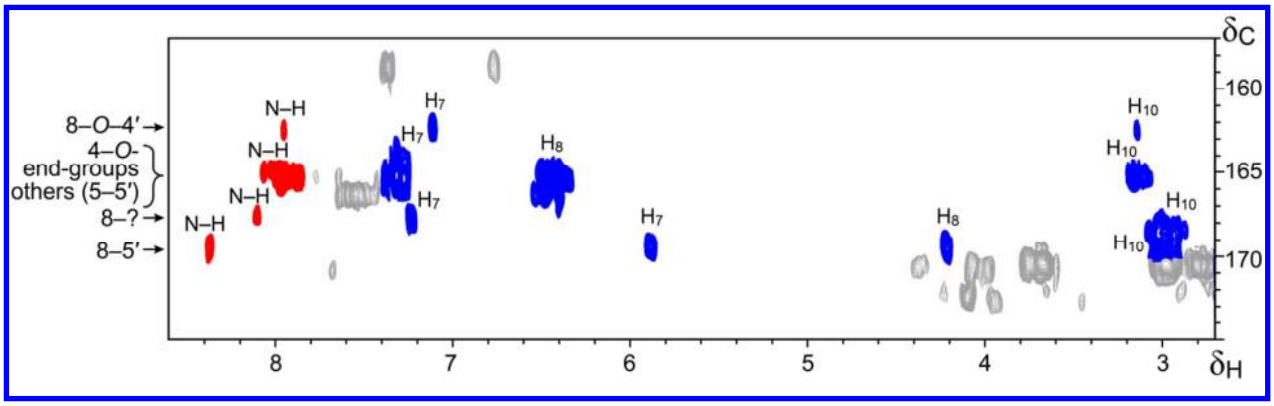
8–O–4′
4–O-
end-groups
others (5–5′)
8–?
8–5′
N–H
N–H
N–H
N–H
H7
H7
H7
H8
H7
H8
H10
H10
H10
H10
δC
160
165
170
8
7
6
5
4
3
δH

Figure 9

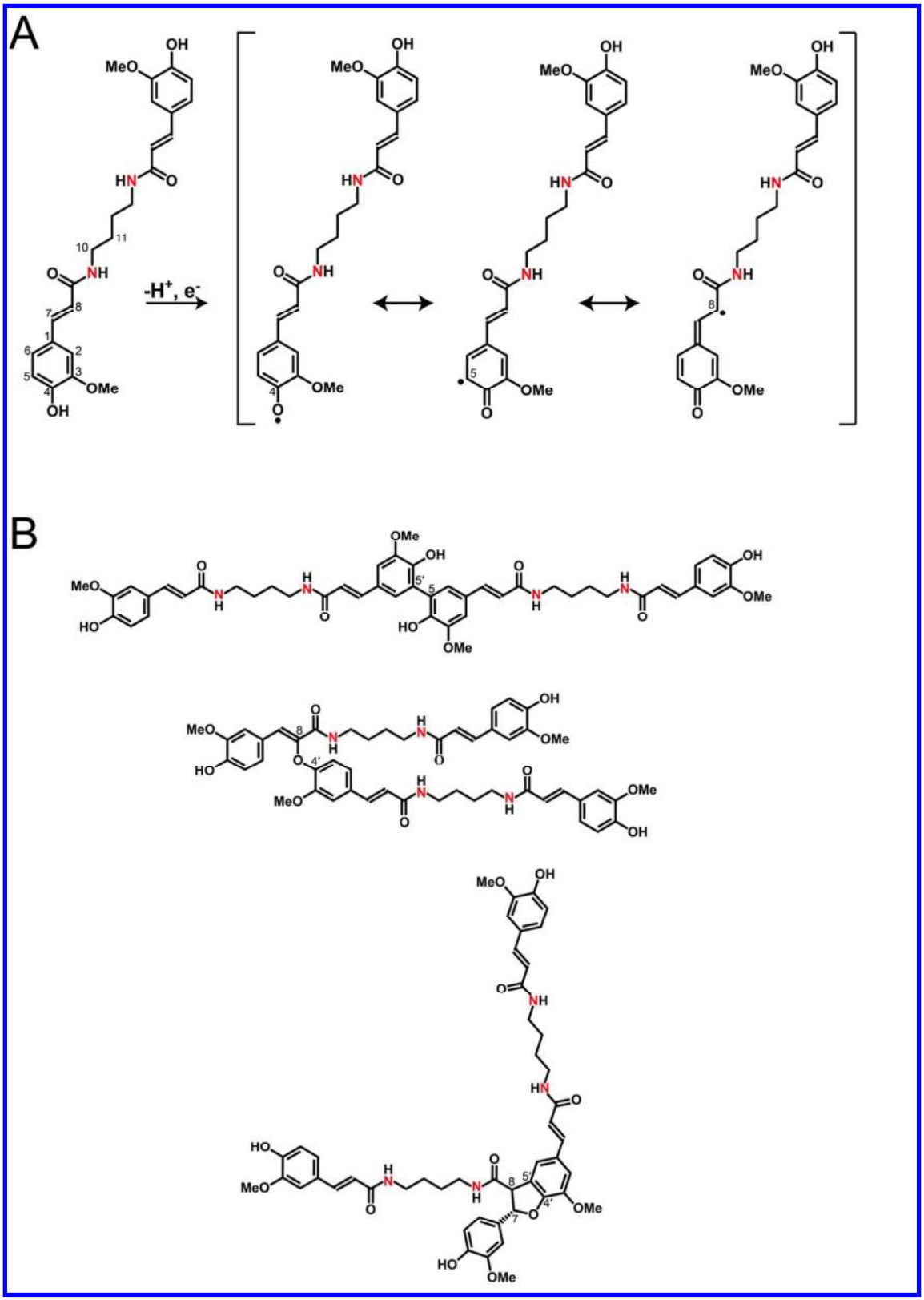

Figure 10

Table of Contents Graphic